1-2003

# Photoinduced Electron-transfer Along Alpha-helical And Coiled-coil Metallopeptides

Anna Fedorova

Anita Chaudhari

Michael Y. Ogawa
*Bowling Green State University - Main Campus*, mogawa@bgsu.edu

J|A|C|S
ARTICLES
Published on Web 12/07/2002

# Photoinduced Electron-Transfer along α-Helical and Coiled-Coil Metallopeptides

Anna Fedorova, Anita Chaudhari, and Michael Y. Ogawa*

*Contribution from the Department of Chemistry and Center for Photochemical Sciences, Bowling Green State University, Bowling Green, Ohio 43403*

Received March 8, 2002; E-mail: mogawa@bgnet.bgsu.edu

***Abstract:*** A peptide-based electron-transfer system has been designed in which the specific positions of redox-active metal complexes appended to either an α-helix, or an α-helical coiled-coil, can be reversed to test the effect of the helix dipole in controlling photoinduced electron-transfer rates. Two 30-residue apopeptides were prepared having the following sequences: (**I**) Ac-K-(IEALEGK)(ICALEGK)(IEALEHK)-(IEALEGK)-G-amide, and (**II**) Ac-K-(IEALEGK)(IHALEGK)−(IEALECK)(IEALEGK)-G-amide. Each apopeptide was reacted first with $[Ru(bpy)_2(phen\text{-}ClAc)]^{2+}$, where bpy = 2,2′-bipyridine and phen-ClAc = 5-chloroacetamido-1,10-phenanthroline, to attach the ruthenium polypyridyl center to the cysteine sidechain of the polypeptide. The isolated products were then reacted with $[Ru(NH_3)_5(H_2O)]^{2+}$ to yield the binuclear electron-transfer metallopeptides **ET-I** and **ET-II**. In these systems, electron-transfer occurred from the photoexcited ruthenium polypyridyl donor to the pentammine ruthenium (III) acceptor such that the electron-transfer occurred toward the negative end of the helix dipole in **ET-I**, and toward the positive end in **ET-II**. Circular dichroism spectroscopy showed that both peptides exist as dimeric α-helical coiled-coils in 100 mM phosphate buffer at pH 7, and as monomeric α-helices in the lower dielectric solvents 2,2,2-trifluoroethanol, and a 1:1 (v/v) mixture of $CH_2Cl_2$ and 2,2,2-trifluoroethanol. The peptides were predominately (i.e., 65−72%) α-helical in these solvents. The emission lifetime behavior of **ET-I** was seen to be identical to that of **ET-II** in each of the three solvents: no evidence for directional electron-transfer rates was observed. Possible reasons for this behavior are discussed.

## Introduction

Studies in the field of de novo protein design have produced new insights into how specific amino acid sequences can fold into predictable and well-defined three-dimensional structures.[1−3] Notable examples of this include the design and synthesis of both parallel[4,5] and antiparallel[6,7] multihelix bundles, in addition to the preparation of multiply stranded β-pleated sheets.[8−11] The results from this and other[12] work provide important illustrations of how protein conformation may be determined by exerting proper control over the hydrophobic, electrostatic, and hydrogen-bond interactions which may occur within a particular amino acid sequence. In recent years, these efforts have been extended to include the study of metalloprotein structures, as various workers have begun to incorporate metal-binding motifs into known examples of de novo designed protein scaffolds.[13,14] An important goal of this research is to understand how the presence of inorganic coordination environments can further influence the conformations of metalloproteins.[15−19]

In addition to providing further insight into the fundamental principles of protein folding, an essential challenge being addressed in the field of de novo protein design is to investigate the ability of rationally designed structural motifs to affect, and perhaps control, the chemical *function* of a synthetic protein.[20] A type of chemical function that is particularly amenable to this type of study is long-range electron-transfer (ET). Indeed, numerous examples now exist in which structure has been shown to influence the ET reactivity of both proteins[21] and

(1) Baltzer, L.; Nilsson, H.; Nilsson, J. *Chem. Rev.* **2001**, *101*, 3153−3163.
(2) DeGrado, W. F.; Summa, C. M.; Pavone, V.; Nastri, F.; Lombardi, A. *Annu. Rev. Biochem.* **1999**, *68*, 779−819.
(3) Baltzer, L. In *Implementation and Redesign of Catalytic Function in Biopolymers*, 1999; Vol. 202, pp 39−76.
(4) Hill, R. B.; Raleigh, D. P.; Lombardi, A.; Degrado, W. F. *Acc. Chem. Res.* **2000**, *33*, 745−754.
(5) Hodges, R. S. *Biochem. Cell Biol.* **1996**, *74*, 133−154.
(6) Oakley, M. G.; Hollenbeck, J. J. *Curr. Opin. Struct. Biol.* **2001**, *11*, 450−457.
(7) Johansson, J. S.; Gibney, B. R.; Skalicky, J. J.; Wand, A. J.; Dutton, P. L. *J. Am. Chem. Soc.* **1978**, *100*, 3881−3886.
(8) Fisk, J. D.; Gellman, S. H. *J. Am. Chem. Soc.* **2001**, *123*, 343−344.
(9) Nesloney, C. L.; Kelly, J. W. *Bioorg. Med. Chem.* **1996**, *4*, 739−766.
(10) Sharman, G. J.; Searle, M. S. *Chem. Commun.* **1997**, 1955−1956.
(11) Sharman, G. J.; Searle, M. S. *J. Am. Chem. Soc.* **1978**, *100*, 5291−5300.
(12) Searle, M. S.; Griffiths-Jones, S. R.; Skinner-Smith, H. *J. Am. Chem. Soc.* **1999**, *121*, 11 615−11 620.
(13) Lu, Y.; Berry, S. M.; Pfister, T. D. *Chem. Rev.* **2001**, *101*, 3047−3080.
(14) Xing, G.; DeRose, V. J. *Curr. Opin. Chem. Biol.* **2001**, *5*, 196−200.
(15) Farrer, B. T.; Harris, N. P.; Balchus, K. E.; Pecoraro, V. L. *Biochemistry* **2001**, *40*, 14 696−14 705.
(16) Dieckmann, G. R.; McRorie, D. K.; Tierney, D. L.; Utschig, L. M.; Singer, C. P.; Ohalloran, T. V.; PennerHahn, J. E.; DeGrado, W. F.; Pecoraro, V. L. *J. Am. Chem. Soc.* **1997**, *119*, 6195−6196.
(17) Laplaza, C. E.; Holm, R. H. *J. Am. Chem. Soc.* **2001**, *123*, 10 255−10 264.
(18) Musgrave, K. B.; Laplaza, C. E.; Holm, R. H.; Hedman, B.; Hodgson, K. O. *J. Am. Chem. Soc.* **2002**, *124*, 3083−3092.
(19) Lombardi, A.; Summa, C. M.; Geremia, S.; Randaccio, L.; Pavone, V.; DeGrado, W. F. *Proc. Natl. Acad. Sci. U. S. A.* **2000**, *97*, 6278−6305.
(20) Baltzer, L.; Nilsson, J. *Curr. Opin. Biotechnol.* **2001**, *12*, 355−360.
(21) Gray, H. B.; di Bilio, A. J.; Farrow, N. A.; Richards, J. H.; Winkler, J. R. *Pure Appl. Chem.* **1999**, *71*, 1753−1764.
(22) Ogawa, M. Y. In *Molecular and Supramolecular Photochemistry*; Ramamurthy, V., Schanze, K. S., Eds.; Marcel Dekker: New York, 1999; Vol. 4, pp 113−150.

peptide-based model systems.[22−27] In the past, discussion of this type of structure−function relationship has focused on understanding the abilities of different protein structures to mediate long-range electronic coupling occurring between distantly located donor and acceptor sites.[28,29] However, several years ago, Fox and co-workers[30−32] reported evidence for an additional way in which a protein structure might be used to regulate the rates of peptide-based electron-transfer reactions. These workers determined that the rates of photoinduced electron-transfer occurring between a *N*,*N*-dimethylanilino donor and a pyrenylalanine acceptor appended to an α-helix were significantly faster when the transfer occurred in the C → N direction rather than in the reverse. From this, it was suggested that the electric field generated by the permanent dipole of α-helices may serve to modulate ET rates in these systems. Thus, it is of interest to see how similar effects can be observed in de novo designed *metallo*proteins as well. Within this context, the α-helical coiled-coil motif has been used by our group to design a new class of model metalloproteins from which the mechanisms of biological electron-transfer reactions can be studied.[23,24,33] The coiled-coil structure consists of a left-handed supercoil of two α-helices and is widely used as an oligomerization domain in native proteins. The model metalloproteins we design employ synthetic coiled-coils to serve as well-defined scaffolds onto which inorganic redox centers can be site-specifically attached. Our studies have previously demonstrated that the coiled-coil motif can be used to design model metalloproteins which can undergo either long-range intra-protein electron-transfer that occur across a noncovalent peptide−peptide interface,[24] or inter-protein electron-transfers whose intermolecular ET rates can be modulated by electrostatic protein−protein interactions.[23] In this paper, we describe a new system in which the specific positions of redox-active metal sites appended to the backbone of a single peptide chain can be reversed to learn more about the ability of the helix dipole to control the rates of photoinduced electron-transfer between two charged metal complexes (Figure 1).

## Materials and Methods

**General Methods.** UV−vis, electrochemical, and circular dichroism (CD) measurements were performed as previously described.[23,24] A 0.1 mm path length cell was used for measuring CD spectra in 1:1 (v/v) mixtures of 2,2,2-trifluorethanol (TFE) and methylene chloride.

Electrospray ionization mass spectra (ESI−MS) were obtained on a Bruker Daltonics Esquire LC−MS at the Department of Chemistry of the University of Toledo, Toledo OH. Cyclic voltammetry was conducted on a BAS 100 W Electrochemical Analyzer using a platinum working electrode, a platinum wire auxiliary electrode, and a Ag/AgCl reference electrode. The instrument was calibrated using an external $Ru(bpy)_3^{2+}$ standard ($E$ = 1.26 V vs NHE).[34]

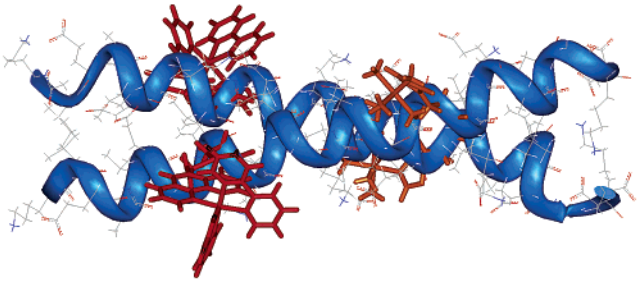

***Figure 1.*** Computer model of the electron-transfer metallopeptide **ET-I**, shown in the coiled-coil conformation.

All peptide metalation reactions were monitored by HPLC on a semipreparative reversed-phase $C_{18}$ column (Zorbax 300SB−$C_{18}$, 9.4 × 250 mm, 5 μm particle size, 300 Å pore size) with an AB gradient of 1% B/min for 20 min followed by a gradient of 0.5% B/min. For both gradients, the flow rate was 2 mL/min and solvent A was 0.1% (v/v) trifluoroacetic acid (HTFA) in water, and solvent B is 0.1% (v/v) HTFA in acetonitrile. Purification of bulk quantities of the peptides was achieved using a preparative $C_{18}$ column (Zorbax 300SB−$C_{18}$, 21 × 250 mm, 7 μm particle size, 300 Å pore size) using the same gradient as described above but at a flow rate of 5 mL/min.

**Peptide Synthesis.** Solid-phase techniques were used to prepare the 30-residue polypeptides, C10H21(30-mer): Ac-K-(IEALEGK)(ICALEGK)(IEALEHK)(IEALEGK)-G-amide (**I**), and H10C21(30-mer): Ac-K-(IEALEGK)(IHALEGK)-(IEALECK)(IEALEGK)-G-amide (**II**), on an Applied Biosystems Model 433A peptide as previously described.[23] ESI−MS *m*/*z* (ion): found for C10H21(30-mer) 1088.2 ([M + 3H$^+$]$^{3+}$), 816.4 ([M + 4H$^+$]$^{4+}$) 653.4 ([M + 5H$^+$]$^{5+}$), 544.6 ([M + 6H$^+$]$^{6+}$; for H10C21(30-mer) 1088.1 ([M + 3H$^+$]$^{3+}$), 816.5 ([M + 4H$^+$]$^{4+}$), 653.3 ([M + 5H$^+$]$^{5+}$), 544.6 ([M + 6H$^+$]$^{6+}$.

**Attachment of the Ruthenium Polypyridyl Center to the Cysteine Side-Chain.** In a typical procedure, a sample of either C10H21(30-mer) or H10C21(30-mer) (5 mg, 1.3 μmol) was dissolved in 1 mL of 100 mM phosphate buffer at pH 7, and the resulting solution was purged with argon gas for 15−20 min. To this was added solid tris-(2-carboxyethyl)phosphine. After stirring under an argon atmosphere for ca. 20 min, the solution was neutralized by the dropwise addition of 1 N NaOH (aq). A solution of $[Ru(bpy)_2(phen\text{-}ClAc)](PF_6)_2$,[33] where bpy = 2,2′-bipyridine and phen-ClAc = 5-chloroacetamido-1,10-phenanthroline, dissolved in a minimum amount of *N*,*N*-dimethylformamide (ca. 0.5 mL) was then added to the reaction mixture. After the mixture was stirred for 4−5 h at room temperature, it was applied directly onto a size-exclusion column (Bio-gel P-2) that was previously equilibrated with 0.1 N HTFA. Elution with the HTFA solution yielded the peptide fraction first followed by the hydrolyzed metal complex. The collected peptide fraction was then analyzed by HPLC and in cases where unreacted apopeptide was detected, the metalation procedure was repeated using a fresh sample of $[Ru(bpy)_2(phen\text{-}ClAc)](PF_6)_2$. The metalated product, [(Ru(bpy)$_2$(phenAc)-C10]H21(30-mer) will hereafter be referred to as **Ru-I**, and the H10[(Ru(bpy)$_2$(phenAc)-C21](30-mer) peptide will be referred to as **Ru-II**. ESI-MS *m*/*z* (ion): found for **Ru-I** 978.2 ([M+4H$^+$]$^{4+}$), 782.7 ([M+5H$^+$]$^{5+}$), 652.5 ([M+6H$^+$]$^{6+}$), 559.5 ([M+7H$^+$]$^{7+}$); for **Ru-II** 978.3 ([M+4H$^+$]$^{4+}$), 782.8 ([M+5H$^+$]$^{5+}$), 652.4 ([M+6H$^+$]$^{6+}$), 559.4 ([M+7H$^+$]$^{7+}$).

**Coordination of the Pentammine Ruthenium Complex to the Histidine Side-Chains.** The Ru(bpy)$_2$(phen)-labeled peptides **Ru-I** and **Ru-II** were metalated at their histidine side-chains by treatment with aquopentammine ruthenium (II) as described previously for the metalation of related coiled-coil peptides.[23,24] However, in the present

(23) Kornilova, A. Y.; Wishart, J. F.; Ogawa, M. Y. *Biochemistry* **2001**, *40*, 12 186−12 192.
(24) Kornilova, A. Y.; Wishart, J. F.; Xiao, W.; Lasey, R. C.; Fedorova, A.; Shin, Y. K.; Ogawa, M. Y. *J. Am. Chem. Soc.* **2000**, *122*, 7999−8006.
(25) Mutz, M. W.; Case, M. A.; Wishart, J. F.; Ghadiri, M. R.; McLendon, G. L. *J. Am. Chem. Soc.* **1999**, *121*, 858−859.
(26) Sasaki, H.; Makino, M.; Sisido, M.; Smith, T. A.; Ghiggino, K. P. *J. Phys. Chem. B* **2001**, *105*, 10 416−10 423.
(27) Sisido, M.; Hoshino, S.; Kusano, H.; Kuragaki, M.; Makino, M.; Sasaki, H.; Smith, T. A.; Ghiggino, K. P. *J. Phys. Chem. B* **2001**, *105*, 10 407−10 415.
(28) Skourtis, S. S.; Beratan, D. N. In *Electron Transfer-from Isolated Molecules to Biomolecules*, *Pt 1*, 1999; Vol. 106, pp 377−452.
(29) Winkler, J. R.; Di Bilio, A. J.; Farrow, N. A.; Richards, J. H.; Gray, H. B. *Pure Appl. Chem.* **1999**, *71*, 1753−1764.
(30) Fox, M. A.; Galoppini, E. *J. Am. Chem. Soc.* **1997**, *119*, 5277−5285.
(31) Galoppini, E.; Fox, M. A. *J. Am. Chem. Soc.* **1996**, *118*, 2299−2300.
(32) Knorr, A.; Galoppini, E.; Fox, M. A. *J. Phys. Org. Chem.* **1997**, *10*, 484−478.
(33) Fedorova, A.; Ogawa, M. Y. *Bioconjugate Chem.* **2002**, *13*, 150−154.
(34) Juris, A.; Balzani, V.; Barigelletti, F.; Campagna, S.; Belser, P.; Vonzelewsky, A. *Coord. Chem. Rev.* **1988**, *84*, 85−277.

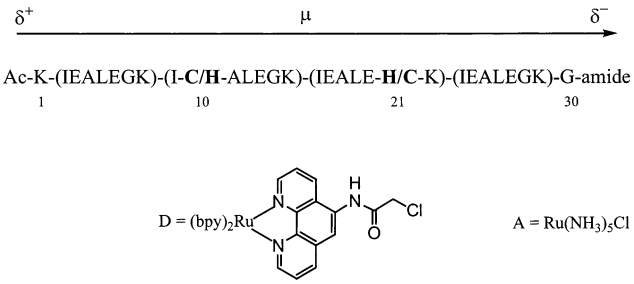


***Figure 2.*** Sequence of apopeptides **I** = C10H21(30-mer) and **II** = H10C21(30-mer). The binuclear ET metallopeptides are prepared by first reacting the ruthenium polypyridyl complex (D) to the cysteine residue of the appropriate peptide and then attaching the pentammine ruthenium species (A) to the histidine residue.

study, the reaction mixtures were treated with 0.1 N HTFA for 2−3 h prior to purification by reversed-phase HPLC to help remove any glutamate-bound ruthenium pentammine species. The binuclear electron-transfer peptides, [(Ru(bpy)$_2$(phenAc)-C10][Ru(NH$_3$)$_5$−H21](30-mer) will hereafter referred to as **ET-I**, and its substitutional isomer, [Ru-(NH$_3$)$_5$−H10][(Ru(bpy)$_2$(phenAc)-C21](30-mer) will be referred to as **ET-II**. ESI−MS *m/z* (ion): found for **ET-I** 1366.5 ([M + 3H$^+$]$^{3+}$), 1024.4 ([M + 4H$^+$]$^{4+}$), 819.9 ([M + 5H$^+$]$^{5+}$); for **ET-II** 1366.1 ([M + 3H$^+$]$^{3+}$), 1024.1 ([M + 4H$^+$]$^{4+}$), 819.8 ([M + 5H$^+$]$^{5+}$).

## Results

**Synthesis and Characterization of the Metallopeptides.** The two 30-residue polypeptides, C10H21(30-mer) (**I**): Ac-K-(IEALEGK)(ICALEGK)(IEALEHK)(IEALEGK)-G-amide, and H10C21(30-mer) (**II**): Ac-K-(IEALEGK)(IHALEGK)-(IEA-LECK)(IEALEGK)-G-amide were prepared by solid-phase techniques, purified by a combination of reverse-phase HPLC and size-exclusion chromatography, and characterized by ESI−MS. The sequence of these peptides (Figure 2) are based upon a seven residue heptad repeat, *(abcdefg)$_n$*, in which positions *a* and *d* are occupied by hydrophobic amino acids, positions *b*, *c*, and *f* are occupied by hydrophilic residues, and positions *e* and *g* are occupied by oppositely charged residues. Such sequences have been designed by Hodges and co-workers[5] to self-assemble into two-stranded, parallel α-helical coiled-coils when dissolved in aqueous solution. Peptides **I** and **II** differed from one another only in their placement of the cysteine and histidine residues along their sequences. This allowed preparation of the desired ET metallopeptides in which the direction of photoinduced electron-transfer can be reversed by switching the position of a cysteine-specific electron-donor and a histidine-specific electron-acceptor in the sequence. As unfolding often occurs at peptide termini, the attachment sites were placed at positions 10 and 21 of the sequence, away from the ends of peptides. Thus, as was described elsewhere,[33] the cysteine residues located at either position 10 or 21 of the peptides were first coupled to a ruthenium tris(polypyridyl) complex by reaction with [Ru(bpy)$_2$-(phen-ClAc)](PF$_6$)$_2$, where phen-ClAc = 5-chloroacetamido-1,10-phenanthroline and bpy = 2,2′-bipyridine, to yield the mononuclear metallopeptides **Ru-I**: [Ru(bpy)$_2$(phenAc)-C10]-H21(30-mer), and **Ru-II**: H10[Ru(bpy)$_2$(phenAc)-C21](30-mer). Molecular modeling studies show that the flexible acetyl linker allows the ruthenium polypyridyl center to sample a variety of positions relative to the helix axis. From this, the range of possible edge-to-backbone distances extends from ca. 3−8 Å.

Treatment of **Ru-I** and **Ru-II** with aquopentammine ruthenium (II) metalated the histidine residues to yield the binuclear peptides [(Ru(bpy)$_2$(phenAc)-C10][Ru(NH$_3$)$_5$−H21](30-mer) called **ET-I**, and [Ru(NH$_3$)$_5$−H10][(Ru(bpy)$_2$(phenAc)−C21]-(30-mer) called **ET-II**. The two binuclear metallopeptides were purified by reverse-phase HPLC and characterized by ESI−MS, as described above. In summary, binuclear metallopeptides were designed such that photoinduced electron-transfer involving a ruthenium polypyridyl excited-state donor and a pentammine ruthenium (III) acceptor will occur in a direction that is toward the negative end of the helix dipole in **ET-I** and toward the positive end in **ET-II**.

The low synthetic yield of **ET-I** and **ET-II**[33] precluded the possibility of measuring their ground-state redox potentials by electrochemical methods. However, previous studies showed that the redox potential of the related Ru(NH$_3$)$_5$−H21(30-mer) peptide was $E$ = 0.065 V vs NHE.[24] Cyclic voltammetry performed on the model compound, [Ru(bpy)$_2$(phen-Ac)]$^{2+}$, where phen-Ac = 5-acetamido-1,10-phenanthroline showed a single, reversible wave at 1.36 V vs NHE in 0.1 M HTFA. The potential of the related compound, [Ru(dmphen)$_2$(phen-AcCl)] was measured to be E = 1.20 V vs NHE, where dmphen = 4,7-dimethyl-1,10-phenanthroline and phen-AcCl = 5-chloro-acetamido-1,10-phenanthroline.

The UV-Vis spectra of both **ET-I** and **ET-II** have maxima at 192, 286, and 451 nm, and can be described as being superpositions of those of the [Ru(bpy)$_2$(phen-ClAc]$^{2+}$ starting material and the relevant apopeptides. The spectral contributions from the ruthenium pentammine centers are negligible due to the relatively low molar absorptivity of these complexes.

**Circular Dichroism Spectroscopy.** The circular dichroism (CD) spectra of apopeptides **I** and **II** both consist of a positive signal at 194 nm and negative bands at 208 and 222 nm which shows that these peptides are α-helical in nature. When measured in 100 mM phosphate buffer (pH 7, 278 K), the molar ellipticities at 222 nm increased in magnitude at higher concentrations to indicate the formation of the coiled-coil conformation.[5] The concentration data accurately follow eq 1

$$K_d = 2[M_0]\,(1-\Delta\theta/\Delta\theta_{max})^2/(\Delta\theta/\Delta\theta_{max}) \qquad (1)$$

which describes a two-state monomer−dimer equilibrium in which [M$_0$] is the total peptide concentration, $\Delta\theta = (\theta_{obs} - \theta_0)$, $\Delta\theta_{max} = (\theta_{max} - \theta_0)$, $\theta_{max}$ is the ellipticity of the folded dimer, and $\theta_0$ is the ellipticity of the unfolded monomer taken to be 2500 deg cm$^2$ dmol$^{-1}$.[35] A nonlinear fit of the data obtained for **II** (not shown) yields values of $K_d$ = 2.0 ± 0.40 $\mu$M and $\theta_{max}$ = −27 900 ± 100 deg cm$^2$ dmol$^{-1}$. Similar results were obtained for **I**. A comparison of the values obtained for $\theta_{max}$ to that calculated for an ideal 30-residue α-helix shows that both peptides **I** and **II** can attain maximum helicities of ca. 81%. These results are consistent with those obtained for related peptides for which the lower helical content was attributed to end-group disorder.[36]

The CD spectra of the binuclear peptides **ET-I** and **ET-II** are nearly identical to those just described for the related apopeptides. The lack of sample availability precluded the

(35) Wendt, H.; Berger, C.; Baici, A.; Thomas, R. M.; Bosshard, H. R. *Biochemistry* **1995**, *34*, 4097−4107.
(36) Su, J. Y.; Hodges, R. S.; Kay, C. M. *Biochemistry* **1994**, *33*, 15 501−15 510.

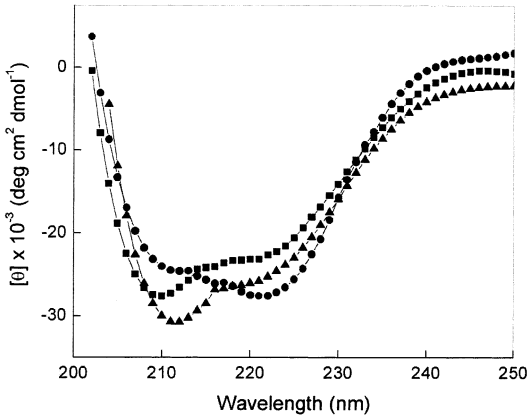


***Figure 3.*** Circular dichroism spectra of the **ET-I** taken in 100 mM phosphate buffer, pH 7 (●); 2,2,2-trifluoroethanol (■); and 1:1 (v/v) 2,2,2-trifluoroethanol:$CH_2Cl_2$ (▲). The spectra were measured at peptide concentrations of 20, 20, and 88 $\mu$M in these solvents, respectively.

possibility of conducting concentration studies on these metallopeptides. However, the spectra obtained for both **ET-I** and **ET-II** at 20 $\mu$M peptide concentration (Figure 3) showed values of $[\theta]_{222}/[\theta]_{208} = 1.05$ in 100 mM phosphate buffer, pH 7. The binuclear metallopeptides thus exist as α-helical coiled-coils under these conditions, and the molar ellipticities measured at 222 nm show that **ET-I** and **ET-II** have helical contents of ca. 80% and 70% respectively, under the conditions used for the electron-transfer experiments described below.

The data presented in Figure 3 show that the conformational properties of **ET-I** and **ET-II** are solvent-dependent. The CD spectra taken in 2,2,2-trifluoroethanol (TFE) have ellipticity ratios of $[\Theta]_{222}/[\Theta]_{208} = 0.85$, which is smaller than those seen in aqueous solution. These results are similar to that reported for related synthetic peptides in which the helix-forming, yet hydrophobic, TFE solvent induces a transition from two-stranded coiled-coils to single-stranded (i.e. monomeric) α-helices.[36,37] Under these conditions, the helical contents of **ET-I** and **ET-II** are measured to be 65% and 75%, respectively. Similar results were observed when spectra were taken in 1:1 (v/v) TFE:$CH_2Cl_2$ as the peptides were also shown to exist as monomeric α-helices. Both ET metallopeptides were ca. 72% helical in this mixed solvent. In summary, CD measurements show that both **ET-I** and **ET-II** exist as two-stranded α-helical coiled-coils in aqueous solution and as monomeric α-helices in 2,2,2-trifluoroethanol and 1:1 (v/v) 2,2,2-trifluorethanol:methylene chloride.

**Photophysical Properties of the Ru-I and Ru-II.** The mononuclear metallopeptides **Ru-I** and **Ru-II** displayed broad emission spectra having maximal amplitudes at 610 nm when dissolved in 100 mM phosphate buffer (pH 7) at ambient temperatures. The spectra became vibrationally resolved, and showed $E^{0-0}$ bands occurring at 580 nm (2.14 eV) when taken in an ethanol-methanol glass (4:1 v/v) at 77 K.

Emission lifetime experiments performed at ambient temperatures in argon-saturated 100 mM phosphate buffer (pH 7) showed that the luminescence of both **Ru-I** and **Ru-II** decayed via

$$I(t) = A_S\exp(-k_S\,t) + A_L\exp(-k_L t) \qquad (2)$$

biexponential kinetics as described by eq 2 in which $A_S$, $k_S$ and $A_L$, $k_L$ are the amplitudes and rate constants for the shorter and longer-lived components, respectively. A nonlinear least-squares fit of the data to eq 2 showed that the longer-lived component comprised approximately 90% of the total emission for both metallopeptides. The lifetimes for the major component were $\tau_L = 1/k_L = 1184 \pm 9$ ns for **Ru-I** and $\tau_L = 1151 \pm 43$ ns for **Ru-II** (Table 1). These values are consistent with the lifetimes reported for similar ruthenium polypyridyl compounds.[34] The minor decay components of **Ru-I** and **Ru-II** had lifetimes of $\tau_s = 150$ ns, and their origin is currently under investigation.

The emission lifetime traces of both **Ru-I** and **Ru-II** were solvent-dependent such that single-exponential kinetics were observed when the metallopeptides were dissolved in either TFE or a 1:1 (v/v) mixture of TFE:$CH_2Cl_2$, solvents in which the peptides were shown to exist as monomeric α-helices by circular dichroism spectroscopy. As shown in Table 1, the lifetimes of the two mononuclear peptides were nearly identical to one another, having values of $\tau \approx 310$ and 205 ns when dissolved in argon-saturated TFE and 1:1 (v/v) TFE:$CH_2Cl_2$, respectively.

**Electron-Transfer Properties of ET-I and ET-II.** When measured in 100 mM phosphate buffer, pH 7, the emission decay profiles for the binuclear derivatives **ET-I** and **ET-II** (Figure 4) differed from those just described for the related donor-only peptides. The decays were considerably more rapid, and whereas the emission from the electron-transfer peptides still followed biexponential decay kinetics, the signals were now dominated by the *shorter* lifetime components (85−90%). By analogy to the results of previous studies,[38] this quenching of the ruthenium polypyridyl luminescence is attributed to an electron-transfer reaction occurring between the photoexcited ruthenium polypyridyl donors and the pentammine ruthenium (III) acceptors. Analyses of the data to eq 2 yielded identical values of $\tau_s = 72 \pm 5$ ns for both **ET-I** and **ET-II**. As these values were independent of peptide concentration within the range examined (3−25 $\mu$M), the quenching process results from an intramolecular electron-transfer event. Analysis of the emission data showed that the lifetimes of the minor decay components were also shortened from those of the parent **Ru-I** and **Ru-II** peptides but varied with sample preparation ($\tau_L < 500$ ns). The source of this component is assigned to the presence of a small population of metallopeptides containing glutamate-bound pentammine ruthenium (III) acceptors which were attached to the surface of the peptide in a nonspecific manner.[33]

The rate constants for the intramolecular electron-transfer reactions occurring in **ET-I** and **ET-II** were calculated according to eq 3 in which $\tau_{obs}$ is the observed emission lifetime of the donor−acceptor

$$k_{et} = (1/\tau_{obs} - 1/\tau_0) \qquad (3)$$

complex, and $\tau_0$ is the lifetime of the unquenched donor-only peptide. Using values of $\tau_{obs} = 72 \pm 5$ ns for both **ET-I** and **ET-II**, and $\tau_0 = 1184 \pm 9$ ns for **Ru-I** and $\tau_0 = 1151 \pm 43$ ns for **Ru-II** gave identical values of $k_{et} = (1.3 \pm 1) \times 10^7\ s^{-1}$ for **ET-I** and **ET-II**, respectively. Thus, the data presented in Table 1 show that the two electron-transfer peptides display identical emission lifetime behavior, and that no evidence for directional electron-transfer rates was observed in aqueous solution.

(37) Myszka, D. G.; Chaiken, I. M. *Biochemistry* **1994**, *33*, 2363−2372.

(38) Winkler, J. R.; Nocera, D. G.; Yocom, K. M.; Bordignon, E.; Gray, H. B. *J. Am. Chem. Soc.* **1982**, *104*, 5778−5800.

***Table 1.*** Luminescence Lifetime Data[a]

| | buffer[b] | | TFE | | TFE:$CH_2Cl_2$ | |
|---|---|---|---|---|---|---|
| | $\tau_S$ (%)[c] ns | $\tau_L$ (%)[c] ns | $\tau_S$ (%)[c] ns | $\tau_L$ (%)[c] ns | $\tau_S$ (%)[c] ns | $\tau_L$ (%)[c] ns |
| Ru−I | 149 ± 6 (8−15) | 1184 ± 9 (85−92) | 309 ± 7 | | 200 ± 7 | |
| ET-I | 72 ± 5 (85−90) | <500[d] (10−15) | 70 ± 2 (65−75) | 253 ± 5 (25−35) | 46 ± 3 (60−80) | 193 ± 20 (20−40) |
| Ru−II | 155 ± 15 (8−15) | 1151 ± 43 (85−92) | 311 ± 8 | | 208 ± 4 | |
| ET-II | 72 ± 5 (85−90) | <500[d] (10−15) | 67 ± 8 (35−45) | 256 ± 9 (55−65) | 59 ± 5 (35−55) | 211 ± 4 (45−65) |

[a] $\tau = 1/k$. [b] 100 mM phosphate buffer, pH 7. [c] Relative weighting of the component. [d] The lifetime and amplitudes of this component vary with sample preparation and is tentatively attributed to the presence of nonspecifically bound pentamminecarboxylatoruthenium(III) impurities on the surface of the peptide.[33]

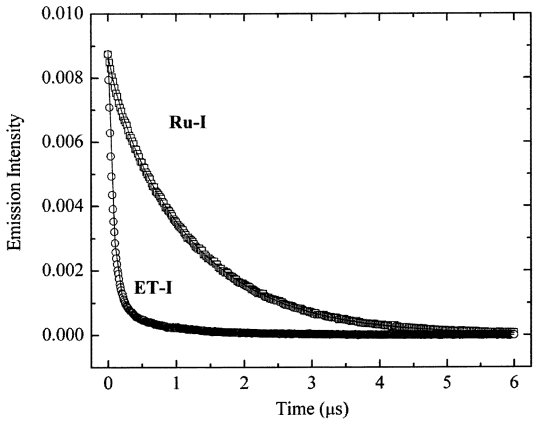


***Figure 4.*** Emission lifetimes of **Ru−I** and **ET-I** measured in 100 mM phosphate buffer (pH 7) at ambient temperatures. The solid lines represent fits of the data to eq 2 as described in the text.

Previous work by the Fox group showed that larger kinetic dipole effects were observed when ET experiments were conducted in solvents of lower dielectric constant.[30,31] It was observed that in methanol ($\epsilon = 36$), a 5-fold rate enhancement was observed when ET was made to occur in the C to N direction rather than in the opposite direction, which increased to a 24-fold difference in directional ET rates when the experiments were conducted in $CH_2Cl_2$ ($\epsilon = 9$). Thus, to further probe for the potential effects of the helix dipole in modulating the electron-transfer rates in **ET-I** and **ET-II**, lifetime experiments were performed in 2,2,2-trifluoroethanol, which has a dielectric constant of $\epsilon = 27$, and in 1:1 (v/v) mixture of 2,2,2-trifluoroethanol and methylene chloride. It is noted that the CD experiments described above showed that both **ET-I** and **ET-II** exist as monomeric α-helices under these conditions.

An examination of the data presented in Table 1 shows that the emission behavior of **ET-I** and **ET-II** are identical to one another in each of these two low dielectric solvents. In TFE, the emission decays followed biexponential kinetics (eq 2) to show the presence of significant populations of quenched and unquenched ruthenium polypyridyl excited-states. This observation suggests the existence of two conformational populations of metallopeptides, each having their metal centers placed at different through-space distances along the α-helical peptide bridge. The lack of quenching in one of these conformations suggests that it positions the redox sites far enough apart to prevent electron-transfer from occurring. Significantly, in the cases where photoinduced electron-transfer does occur, analysis of the data according to eq 3 gave identical values of $k_{et} = (1.2 \pm 0.1) \times 10^7\ s^{-1}$ for both **ET-I** and **ET-II**. Similar behavior was observed when the experiments were performed in TFE: $CH_2Cl_2$. The peptides had nearly identical emission lifetimes which yielded similar values of $k_{et} = (1.7 \pm 0.1) \times 10^7\ s^{-1}$ and $k_{et} = (1.2 \pm 0.1) \times 10^7\ s^{-1}$ for **ET-I** and **ET-II**, respectively. Thus, no significant difference in intramolecular electron-transfer rates was observed between these two peptides in the low dielectric solvents.

## Discussion

The metallopeptides **ET-I** and **ET-II** were designed to study if the electric field generated by the dipole of an α-helix can be used to control the rates of photoinduced electron-transfer occurring between two pendant metal complexes. In contrast to the results of previous studies involving organic donors and acceptors,[30−32] no evidence for directional electron-transfer rates was observed for the current system when the experiments were performed in solvents of either high, or low dielectric constant.

Semiclassical Marcus theory[39] can be used to further elucidate the electron-transfer properties of **ET-I** and **ET-II**. According to this model, the rates of intramolecular ET reactions can be described by

$$k_{et} = \sqrt{\frac{4\pi^3}{h^2 \lambda k_B T}}\, H_{DA}^2 \exp\left(\frac{-(\Delta G^\circ + \lambda)^2}{4\lambda k_B T}\right) \qquad (4)$$

eq 4 in which the magnitude of $k_{et}$ is controlled by the interplay between the thermodynamic driving force ($-\Delta G^\circ$) and reorganization energy ($\lambda$) for the reaction. $H_{DA}(r)$ is the electronic coupling matrix element which describes how these rates also depend on the strength of the electronic interaction between the donor and acceptor sites. Thus, for a given donor−acceptor separation, values of $k_{et}$ will increase with increasing driving force until reaching a maximum value at $\Delta G^\circ = -\lambda$. From this, it is evident that electron-transfer rates will be most sensitive to changes in driving force under conditions where $-\Delta G^0 \neq \lambda$, and it is within these regimes that the effects of the helix dipole moment should be most easily detected.

The thermodynamic driving force for electron-transfer occurring from a photoexcited electron donor (D*) to an electron-acceptor (A) can be calculated according to eq 5 in which $E_{1/2}(D/D^+)$ is the

$$\Delta G_{et} = [E_{1/2}(D/D^+) - E^{0-0}(D)] - E_{1/2}(A/A^-) \qquad (5)$$

halfwave potential for the oxidation of the donor, $E_{1/2}(A/A^-)$ is the halfwave potential for the reduction of acceptor, and $E^{0-0}(D)$ is the excited-state energy of the donor. Using values of $E^{0-0}(D) = 2.14$ eV taken from the 77 K emission spectrum of **Ru-I** and **Ru-II**, and $E_{1/2}(D/D^+) = 1.36$ V vs NHE taken from the value measured for the model compound [Ru(bpy)$_2$-

(39) Marcus, R. A.; Sutin, N. *Biochim. Biophys. Acta* **1985**, *811*, 265−322.

(phen-Ac)]$^{2+}$, and $E_{1/2}(A/A^-) = 0.07$ V vs NHE as taken from the electrochemistry of a related coiled-coil metalloprotein,[23,24] gives an estimated value of $\Delta G_{et} = -0.85$ eV for the donor−acceptor peptides **ET-I** and **ET-II**.

An approximate value for the reorganization energy, $\lambda_{12}$, can be obtained from the Marcus cross relation (eq 6)

$$\lambda_{12} = 1/2\,[\lambda_{11} + \lambda_{22}] \quad (6)$$

where $\lambda_{11}$ and $\lambda_{22}$ are the self-exchange reorganization energies for the donor and acceptor species, respectively. Substitution of the previously reported[40,41] values of $\lambda_{11} = 0.6$ eV for Ru(bpy)$_3$, and $\lambda_{22} = 1.20$ eV for Ru(NH$_3$)$_5$pyr yields a value of $\lambda_{12} = 0.9$ eV. From these calculations, it appears that the photoinduced electron-transfer reactions occurring in **ET-I** and **ET-II** will occur toward the top of the Marcus curve and may have rates that will be relatively insensitive to changes in driving force. To test this prediction, an analogue to **ET-II** was prepared in which the two 2,2′-bipyridyl ligands of the ruthenium polypyridyl center were replaced by 4,7-dimethyl-1,10-phenanthroline to yield the ET derivative **ET(dmphen)-II**. The redox potential of its relevant model compound, [Ru(dmphen)$_2$(phen-AcCl)], was lowered to $E = 1.20$ V by the presence of the electron-donating methyl groups on the 1,10-phenanthroline ligand. The emission from the mononuclear parent peptide decayed via single-exponential kinetics to give a lifetime of 1.55 $\mu$s. Upon introduction of the ruthenium pentammine acceptor, the lifetime became shortened and followed biexponential kinetics. The dominant component comprised 80% of the decay and had a lifetime of 170 ns. The minor component had a lifetime of 660 ns. Assuming that the minor component is due to the presence of carboxylate-bound ruthenium pentammine impurities as described above, a value of $k_{et} = 5.2 \times 10^6$ s$^{-1}$ was obtained for **ET(dmphen)-II** which is 2.5-fold smaller than that measured for **ET-II**. These results show that the rates of electron-transfer occurring in this system are indeed driving-force dependent, and that these reactions occur within the inverted Marcus regime. However, it is also possible that the slower ET rate seen in **ET(dmphen)-II** may be due to other unknown factors, such as a slightly longer donor−acceptor distance. Nevertheless, the available results indicate that the absence of directional electron-transfer rates in **ET-I** and **ET-II** is *not* due to the high driving force of these reactions.

(40) Brown, G. M.; Sutin, N. *J. Am. Chem. Soc.* **1979**, *101*, 883−892.
(41) Chang, I. J.; Gray, H. B.; Winkler, J. R. *J. Am. Chem. Soc.* **1991**, *113*, 7056−7057.

In summary, the metallopeptides **ET-I** and **ET-II** show no evidence for the occurrence of directional electron-transfer rates resulting from the electric field of the helix dipole in aqueous solution, TFE, or a 1:1 (v/v) mixture of $CH_2Cl_2$:TFE, solvents in which the peptides were shown to exist as either two-stranded α-helical coiled-coils or as monomeric α-helices. This behavior is in marked contrast to that observed for the systems studied by Fox and co-workers in which directional ET rates were observed for *N*,*N*-dimethylanilino donors and pyrenyl acceptors appended to α-helical peptides. Whereas, the reason for this apparent discrepancy is presently not understood, important differences do exist between the two systems studied. First, whereas the earlier work examined the rates of photoinduced electron-transfer occurring between nonpolar redox centers, the peptides **ET-I** and **ET-II** employ charged, divalent and trivalent, metal complexes as their donor and acceptor sites. It is possible that the electrostatic effects generated by the presence of these charged complexes may dominate over those exerted by the helix dipole. Second, the metallopeptide systems use a flexible acetyl linker to attach the ruthenium polypyridyl complex to the peptide chain which can place this redox site at distances ranging from ca. 3−8 Å away from the helix axis (edge-to-backbone). This may also serve to reduce the effects of the helix dipole in regulating ET rates. Third, to minimize potential complications arising from the known conformational flexibility of peptide termini, the donor and acceptor sites in **ET-I** and **ET-II** were positioned within the second heptad away from the ends of the sequence. In contrast, the earlier work had its redox sites located closer to the peptide termini. Thus, to determine if any of these factors contribute to the absence of a helix dipole effect, studies are currently underway to design systems which use redox sites that consist of neutral metal complexes, which do not require the use of an acetyl linker, and which can be placed at different regions of the sequence. This work will help elucidate the necessary requirements for allowing the helix dipole moment to regulate electron-transfer rates in *de novo* designed metallopeptides and metalloproteins.

**Acknowledgment.** The authors would like to thank Professors F. Castellano and M. Funk for use of the laser and mass spectral facilities, respectively. Electrochemical measurements were performed by Mr. Liu Liu. This work was supported by the National Institutes of Health through Grant No. R01 GM61171 and the Petroleum Research Fund through Grant No. 34901-A.C. A.F. gratefully acknowledges receipt of a predoctoral fellowship from the Harold and Helen McMaster Foundation.

JA026140L